NJC

Accepted Manuscript

This is an *Accepted Manuscript*, which has been through the Royal Society of Chemistry peer review process and has been accepted for publication.

Accepted Manuscripts are published online shortly after acceptance, before technical editing, formatting and proof reading. Using this free service, authors can make their results available to the community, in citable form, before we publish the edited article. We will replace this *Accepted Manuscript* with the edited and formatted *Advance Article* as soon as it is available.

You can find more information about *Accepted Manuscripts* in the Information for Authors.

Please note that technical editing may introduce minor changes to the text and/or graphics, which may alter content. The journal's standard Terms & Conditions and the Ethical guidelines still apply. In no event shall the Royal Society of Chemistry be held responsible for any errors or omissions in this *Accepted Manuscript* or any consequences arising from the use of any information it contains.

ROYAL SOCIETY OF CHEMISTRY

www.rsc.org/njc

Effect of microwave irradiation time and temperature on the spectroscopic and morphological properties of nanostructured poly(carbazole) synthesized within bentonite clay galleries

Ufana Riaz*, S.M.Ashraf[+], and Ashima Madan
Materials Research Laboratory, Department of Chemistry,
Jamia Millia Islamia (A Central University), New Delhi-110025, India
*Corresponding author: Fax-(+91-112-684-0229); *E-mail address*- (ufana2002@yahoo.co.in)
[+] Now retired

Abstract

Microwave irradiation has been widely used in the synthesis of organic, inorganic, and inorganic-organic hybrid materials because of its well known advantages over conventional synthetic routes. Polycarbazole (PCz) is a hole transporting conducting polymer and by virtue of this property is attracting considerable attention for its application in organic light emitting diodes (OLEDs) and solar cells. For advanced technologies, PCz of controlled morphology, nano dimension, and higher optoelectronic properties is looked for. These objectives are achievable through using innovative synthetic routes. Towards this end, we have attempted to synthesize PCz under solid state conditions in the confined environment of interlayer space of Bentonite clay through microwave irradiation with ammonium persulphate as initiator. The effect of time and temperature of microwave irradiation on the shape, size, molar mass, UV-vis and fluorescence characteristics of PCz and PCz-clay nanohybrids have been thoroughly investigated and interpreted. The temperature of microwave irradiation was from 30 to 50^0C and time was varied from 2 to 6 min. The effect of both temperature and time of microwave irradiation on the synthesized nanocomposite was investigated by FT-IR, UV, XRD techniques. PCz extracted from clay galleries exhibited spherical shape under all conditions of synthesis. The size of spheres, in the nanosize domain, was found to be dependant upon the temperature and time of microwave irradiation. UV-vis spectral analysis showed that microwave irradiation produced polaronic state in PCz like cyclic voltammetry (CV). Oscillator strength of the polaronic transition was noticeably enhanced with temperature and time of microwave irradiation. FT-IR analysis revealed that PCz formed spiral shaped particles within clay galleries. Time and temperature of microwave irradiation was found to significantly enhance the fluorescence intensity of PCz-Bentonite nanocomposites; thus the HOMO and LUMO orbitals of PCz are favorably perturbed by microwave irradiation in a significant measure. Enhancement of optoelectronic parameters of microwave synthesized PCz is expected to drastically improve the quantum efficiency of OLEDs and power efficiency of organic solar cells.

Introduction

Microwave-assisted synthesis has attracted wider attention of the scientist as this technique provides far faster, cleaner, economic and controllable green route for synthesizing all types of organic compounds and numerous technologically important inorganic materials[1-4]. New microwave synthesizers having precise temperature and pressure control have helped the synthesis of polymers of different types with better structure control [5-6]. This has opened the opportunity to synthesize organic-inorganic hybrid materials through microwave irradiation. Recent progress in the synthesis of in inorganic-organic hybrid materials through conventional heating methods has led to the development of novel technological materials of enormous significance [6].Layered metal hydroxide, clays and silica, and other mesoporous inorganic materials have been extensively investigated as inorganic host for many organic materials as guest for developing hybrid materials for advanced technologies [7-13].

Conducting polymers are well recognized for showing electronic conductivity and semi-conductivity, redox behavior, electrochromism and photochromism, UV-visible light absorbance, and fluorescence. These properties have been variously used in thin solid state batteries, organic light emitting diodes (OLEDs), organic solar cells, electrochromic displays and chemical and biosensors[14]. All these applications have limitations of efficiency which are the subject of vigorous research for improvement.

Smectite clays have layered silicate structures which have aluminium or magnesium oxide octhedra sandwiched between two silicon oxide tetrahera with a gallery between two such siloxane layers. An infinite number of such layers and interlayer galleries are stacked in the c-direction of the crystal structure of smectite. The siloxane layers have negative charge which is compensated by the mono and divalent cations present in the interlayer space surrounded by an aqueous layer[15]. The gallery in the smectite structure has compatible height of ≈ 1.4 nm and many organic moieties can be intercalated in the interlayer space to obtain organic–inorganic hybrid materials[16]. *Rui-Hitzky et.al.*[17-18] have intensively investigated the intercalation of polyethylene oxide by several methods including microwave irradiation. PEO-smectite nanohybrid synthesized by microwave irradiation yielded highest ionic conductivity[19]. Conducting polymer-clay nanohybrids have also been extensively studied. Polycarbazole (PCz) is a conducting polymer which is distinguished by its hole cconducting characteristics.It thus holds potential for application in LEDs, OFETs, and solar cells[20]. Carbazole (Cz) is amenable to chemical modification through substitution at the nitrogen in the pyrrole unit and at selected positions on the benzene rings.The electronic and optical properties of PCz can therefore be be modified to the best advantage. Several authors have extensively worked on the chemical modification of carbazole to enhance the functional characteristics of PCz [21-25]. Only scant literature is available on the controlled morphological aspect of PCz. Riaz and Ashraf[26] have studied the intercalation and polymerization of Cz in bentonite clay galleries using $FeCl_3$ as an oxidant and have found respectively rod and cucumber shaped microstructure of variable dimension at higher and lower loading of PCz in the galleries, with higher values of oscillator strength and quantum yield at lower loading of PCz. It is hoped that polymerization of Cz through microwave irradiation with chosen initiator under conditions of different time and temperature of synthesis in smectite clay galleries can lead to the growth of controlled microstructure of PCz. It can also reveal the enhancing effect of microwave irradiations on electronic, optical and optoelectronic properties of PCz, and its nanohybrid with smectite clays. Clay can acquire multifunctionality in this process. These properties can spur the application of the aforementioned materials in advancesd technologies. To explore the above aspects in depth we have synthhesized PCz-Bentonite nanohybrids by solid state polymerisation and intercalation effected by microwave irradiation for three different times, 2 min, 4 min, and 6 min and at three different temperatures, 30^0C, 40^0C, and 50^0C with ammonium persulphte as initiator. The suitable gallery height, high aspect ratio, and natural abundance prompted the choice of bentonite clay as inorganic host. The synthesized nanohybrids were deeply investigated by FT-IR, UV-visible, and fluorescence spectroscopies; molar mass determination, TGA, XRD, and TEM microscopy to bring forth the effect of temperature and time of irradiation on the electronic, spectroscopic, fluorescence, and microstructural characteristics of these nanohybrids.

Experimental

Materials

Bentonite (Sigma Aldrich, USA), Carbazole (Sigma Aldrich, USA), ammonium per sulphate $(NH_4)_2S_2O_8$)(Merck, India), were used without further purification.

Synthesis of Bentonite/PCz nanocomposites

Bentonite clay (1g) was mixed with carbazole (Cz) (0.5g) using agate mortar rand pestle.The mole ratio of oxidant (ammonium persulphate):carbazole was taken to be 1:1. The microwave irradiation was carried out for 2, 4, and 6 min in Ladd Research Laboratory microwave oven model LBP125-230 (220/230V), power source- 230 V ~50 Hz, energy output- 800 W; input power-1,200 W). During micro wave synthesis, the color of bentonite clay changed from cream to green which indicated the polymerization of carbazole within the bentonite galleries. The nanohybrids obtained were then repeatedly washed with distilled water and methanol, dried in vacuum oven at 70^0C for 72 hours to ensure complete removal of impurities, solvent and water. The colour of the nanocomposites obtained in these cases was found to be green. The nanocomposites were designated as 2min-30^0C-BT/PCz, 4min-30^0C-BT/PCz, and 6min-30^0C-BT/PCz, 2min-40^0C-BT/PCz, 4min-40^0C-BT/PCz , 6min-40^0C-BT/PCz and as 2min-50^0C-BT/PCz, 4min-50^0C-BT/PCz and 6min-50^0C-BT/PCz after the time and temperature of irradiation used in the microwave assisted synthesis .

Characterization

FT-IR spectra of nanohybrids were taken on Perkin-Elmer 1750, FTIR spectrophotometer (Perkin Elmer Instruments, Norwalk, CT) in the form of KBR pellets.

UV-visible spectra were taken on UV-visible spectrophotometer model Shimadzu UV-1800 using NMP as solvent.

The percent loading pf PCz in bentonite was determined using thermogravimetric analyzer (TGA) model EXSTAR TG/DTA 6000 121 under nitrogen atmosphere at a heating rate of 10ºC/min. Molar mass was determined using gel permeation chromatography (GPC). PCz present in the bentonite galleries was extracted by refluxing the polymer/clay nanocomposite in methanol/LiCl by a reported method [27]. GPC measurements were carried out on a Viscotek GPC Max AUTO sampler system consisting of a pump, a Viscotek UV detector and a Viscotek differential refractive index (RI) detector, column (PL1110-6525), pore size 500 (Å), molecular weight range 500-25,000 g/mol polystyrene (PS).THF was used as an eluent at a flow rate of 1.0 mL/min at 30^0C. The data was analyzed using Viscotek OmniSEC Omni-01 software. Transmission electron micrographs (TEM) were taken on Morgagni 268-D TEM, FEI, USA. X-ray diffraction patterns of the nanohybrids were recorded on Philips PW 3710 powder diffractometer (Nickel filtered copper Ka radiations).

The oscillator strength was calculated using the equation:

$$f = 4.32x10^{-9}\int \varepsilon d\bar{\nu} = 4.32x10^{-9}\int \frac{ad\nu}{M}$$

where ε is the molar absorption coefficient , a and M are respectively absorption coefficient at the wavelength in question, and molarity of the PCz solution. In precision analytical determinations integrated absorption coefficient is used in place

of absorption coefficient at the maximum wavelength, λ_{max}. $\int a d\bar{\nu}$ was obtained from the area under the transition peak when the spectra was plotted as absorption coefficient vs. wave number. The area under the peak was obtained using Origin 6.1 which was standardized to Gaussian Lorentzian shape.

Results and discussion

As UV spectra did not reveal the presence of Cz monomer, the weight loss in TGA was attributed to the decomposition of PCz. The percent loading of PCz in the clay galleries at different times and temperatures as calculated by TGA therrmograms is shown in Table 1[28]. Percent polymerization of Cz was then calculated with respect to the monomer concentration initially taken (33%) in the nanocomposite formulation. As the microwave irradiation time increased from 2 min to 6 min at any temperature, the percent conversion of Cz into PCz also increased. At 30^0C, the percent conversion was 72.70%, 76% and 81% for 2, 4 and 6 min irradiation times respectively. At 50^0C and microwave irradiation times 2 min, 4 min, and 6 min, percent conversion of 80%, 82%, and 86 % respectively were obtained. The above results showed that the microwave irradiation caused very fast polymerization; in 2 min at 30^0C; 73% Cz turned into PCz within Bentonite clay galleries. The following sections show that the Bentonite/PCz nanohybrid yielded controlled microstructure and enhanced optical and electronic properties.

Table 1 Percent polymerization of Cz into PCz in Bentonite galleries

Nanocomposite	Bentonite/PCz ratio	% loading*	% polymerization
2 min-30^0C- BT/PCz	1:0.5	24.0	72.70
4 min -30^0C- BT/PCz	1:0.5	25.2	75.90
6 min -30^0C- BT/PCz	1:0.5	27.0	81.10
2 min -40^0C- BT/PCz	1:0.5	26.2	78.90
4 min -40^0C- BT/PCz	1:0.5	26.5	80.48
6 min -40^0C- BT/PCz	1:0.5	28.0	84.68
2 min -50^0C- BT/PCz	1:0.5	26.4	79.87
4 min -50^0C- BT/PCz	1:0.5	27.2	82.28
6 min -50^0C- BT/PCz	1:0.5	28.4	86.10

*Determined by TGA

TEM micrographs of PCz extracted from Bentonite/PCz nanocomposites synthesized at 30, 40, and 50^0C for 2, 4, and 6 min irradiations were shown in Fig.1. The micrographs all showed spherical particles of varying sizes. In the FT-IR section, we have attempted to explain the formation of PCz spirals within the clay galleries from the integrated absorption coefficient of FT-IR peaks of NH vibrations of PCz molecules. On extraction from the clay galleries the PCz spirals reorganized themselves into spheres. The size of the PCz spheres, therefore, cannot be precisely correlated to the nanocomposite samples from which they were extracted.

The size of molecular chains and the solvent used for extraction influenced the size of the spherical particles outside clay galleries. It was observed that in the composites 2 min-30^0C-BT/PCz, Fig.1(a), 2 min-50^0C-BT/PCz, Fig.1(b), 4 min-30^0C-BT/PCz, Fig.1(c), and 6 min-40^0C-BT/PCz, Fig.1(e) , the particle size varied between 150/200 nm to 300/350 nm. Only in the nanocomposites 4 min-50^0C-BT/PCz,Fig.1(d) and 6 min-$50\ ^0$C-BT/PCz,Fig.1(f), the particle size was found to vary predominantly between 300 nm–500 nm. In the nanocomposite 2 min-30^0C-BT/PCz, Fig.1(a), the particle size varied between 50-90 nm.

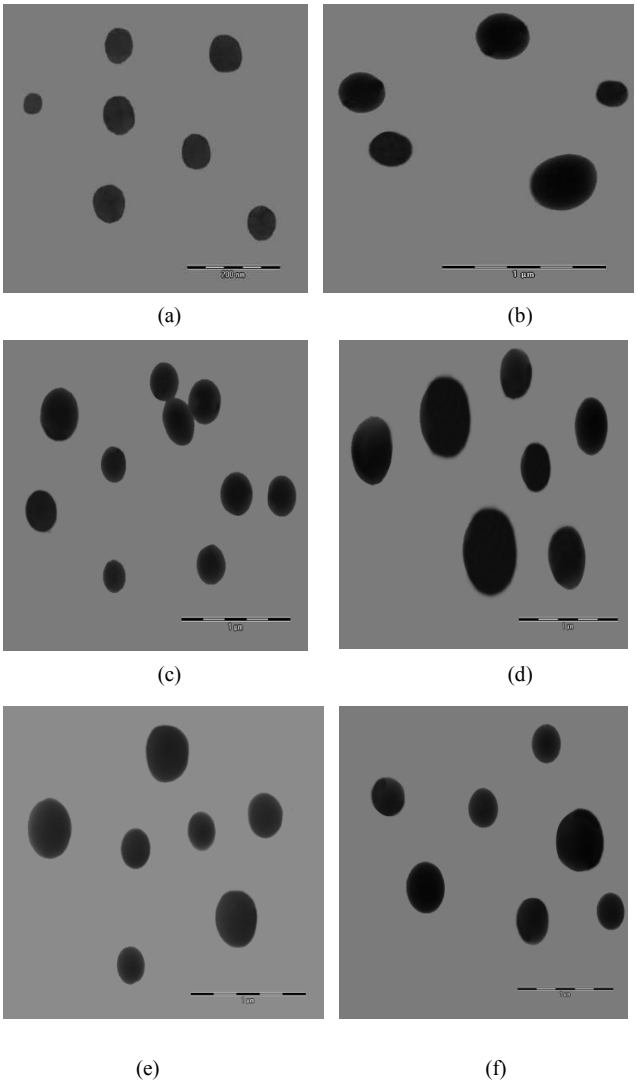

Fig.1 TEM micrographs of (a) 2 min -30^0C-BT/PCz ,(b) 2 min -50^0C-BT/PCz, (c) 4 min -30^0C-BT/PCz (d) 4 min-50^0C-BT/PCz (e) 6 min -40^0C-BT/PCz (f) 6 min -50^0C-BT/PCz

At 30 ^{0}C for 2 min microwave irradiation, PCz particles are of comparatively low molar mass and hence have smaller chains that yield particles of smaller size. The larger size of the particles of the nanocomposites 4min-50^0C-BT/PCz and 6 min-50 ^{0}C-BT/PCz results from the higher molar mass/larger chain size of these nanocomposites, Table 2.

Table 2 Particle size of the nanocomposites

Nanocomposites	Particle size range (nm)
2min-30^{0}C-BT/PCz	50-90
2min-40^{0}C-BT/PCz	150-300
2min-50^{0}C-BT/PCz	150-350
4min-30^{0}C-BT/PCz	200-300
4min-40^{0}C-BT/PCz	200-300
4min-50^{0}C-BT/PCz	300-500
6min-30 ^{0}C-B/PCz	200-350
6min-40^{0}C-BT/PCz	200-375
6min-50^{0}C-BT/PCz	300-450

The larger size of the PCz particles of the nanocomposites 4min-50^{0}C BT/PCz and 6min-50 ^{0}C BT/PCz indicates the effect of higher temperature and higher time of irradiation on the molar mass of the PCz particles formed inside the clay galleries. This is also corroborated by the higher molar mass obtained experimentally for these nanocomposites. Since for 2 min irradiation at 50^{0}C, the particle size is not as large as in the above cases, the time of irradiation in addition to temperature has a significant effect on the molar mass of the PCz grown in the clay galleries.

Molar mass of PCz extracted from the clay galleries of all the nanocomposites were determined as mentioned in the experimental section. We found three ranges of molar mass of PCz extracted from the nanocomposites. 2min-30^{0}C-BT/PCz gave molar mass of 3150 Da. Molar mass of the PCz extracted from the composites 2min-40^{0}C-BT/PCz, 2min-50^{0}C-BT/PCz, 4min- 30^{0}C-BT/PCz, 4min-40^{0}C-BT/PCz , 6min-30^{0}C-BT/PCz, 6min-40 ^{0}C BT/PCz , gave molar mass values in the range of 3445-3545 Da. The PCz taken out from 4min- 50^{0}C-BT/PCz and 6-min 50^{0}C-BT/PCz gave molar mass values of 4058 Da and 3888 Da.It was observed that the PCz formed at 2min-30^{0}C-BT/PCz gave lowest molar mass. Although % conversion was quite high ≈ 73% in this case, but the chain size were smaller because of low molar mass and formation in shorter time. Smaller size of PCz particles at this temperature and time, as was observed in the preceding section, matched with this value of molar mass. The largest particle size of PCz obtained from nanocomposite: 4min-50^{0}C-BT/PCz and 6min-50^{0}C-BT/PCz between 300 nm-450/500 nm also correlated with the highest molar mass of these PCz. The particle size of PCz extracted from the composites 2 min-40^{0}C-BT/PCz, 2min-50^{0}C-BT/PCz, 4min-30^{0}C-BT/PCz and 4min-40^{0}C-B/PCz ,6min- 30^{0}C-B/PCz and 6min-40^{0}C-BT/PCz in the range of 150/200 nm- 300 nm matched to the intermediate values of the molar mass of these PCzs. The largest chain size and molar mass were obtained at 50^{0}C for 4 min or longer microwave irradiation. The lowest chain size was obtained at 30^{0}C for 2 min irradiation. PCz formed under other conditions of temperature and time of irradiation led to intermediate chain size. It was thus observed that the PCz synthesized through microwave irradiation under the above experimental conditions yielded spherical particles of controlled size.

The XRD data of the BT/PCz nanocomposite prepared by microwave irradiation at different times and temperatures are shown in Table 3. It iwas observed that on the polymerization and intercalation of PCz in the Bentonite galleries, the Bentonite peak at 2θ= 5.7^0, shifted to 5.3^0, 5.0^0 and 4.9^0 in the nanocomposites 2min-30^{0}C-BT/PCz, 2min-40^{0}C-BT/PCz, and 2min-50^{0}C-BT/PCz with corresponding gallery heights of 16.5 Å, 17.5 Å, 18.0 Å respectively, vis a vis 15.5 Å gallery height of pure Bentonite. This clearly established the formation of PCz within the clay galleries which pushed the height of the latter upwards. In the section on FT-IR, we have established from the integrated absorption coefficient, $\int adv$, of NH vibration peak of PCz that the chains of the latter took the shape of spirals.

Table 3 Peak analysis data of XRD of BT/PCz nanocomposites

Nanocomposite	Peak position (2θ)	Gallery height (Å)	Intensity (cps)
2min- 30^{0}C-BT/PCz	5.3	16.5	4305
2min- 40^{0}C-BT/PCz	5.0	17.5	3796
2min- 50^{0}C-BT/PCz	4.9	18.0	1667
4min- 30^{0}C-BT/PCz	4.8	18.5	11667
4min- 40^{0}C-BT/PCz	4.9	18.0	5995
4min -50^{0}C-BT/PCz	5.0	17.5	1820
6min- 30^{0}C-BT/PCz	4.2	21.0	100
6min- 40^{0}C-BT/PCz	4.2	21.0	125
6min- 50^{0}C-BT/PCz	5.2	17.0	225

The different values of the gallery height indicated different orientation of PCz spirals. The vertical orientation yielded highest gallery height; the tilted orientation produced the lowest. The lateral orientation were not able to push the gallery height. The mixed orientation of vertical and tilted orientation would produce intermediate values of the gallery height. The highest gallery height was observed for the nanohybrid 6min-30^{0}C-BT/PCz, 21 Å, and lowest for the nanohybrid 2min-30^{0}C-BT/PCz, 16.5 Å. PCz spirals in the former were oriented vertically and in the latter had tilted orientation. The gallery height of other nanohybrids were higher than the latter but lower than 21.0 Å which indicated mixed orientations of PCz particles in the interlayer space of those nanohybrids. These observations match with the results of integrated absorption coefficient in the FTIR section. The microwave irradiation at 50^{0}C for 2, 4, and 6 min yielded the gallery height as 18.0, 17.5 and 17.0 Å indicating that increase in the time of irradiation at this temperature tilted the spirals from mixed orientation to slanting one. But at 30 and 40^{0}C, behavior is the reverse; the gallery height was found to increase as the irradiation time was increased from 2min to 4min to 6 min.(Table 3). It appears that at 30^{0}C and 40^{0}C the increase in irradiation time tilts the orientation from slanting to mixed and vertical one.

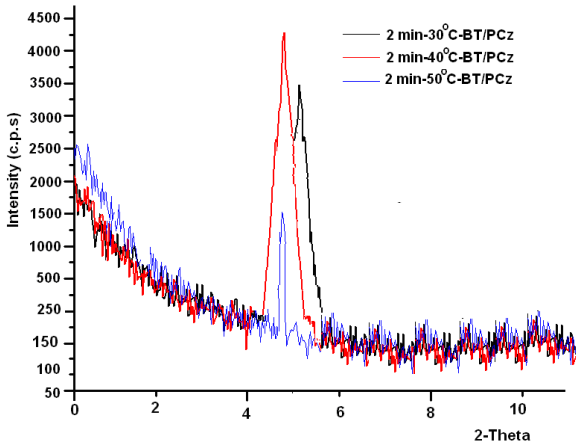

(a)

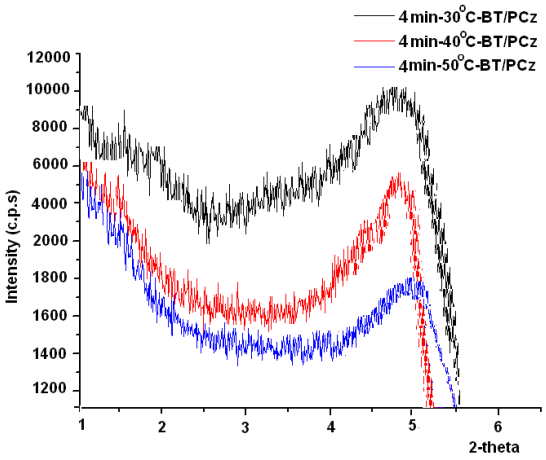

(b)

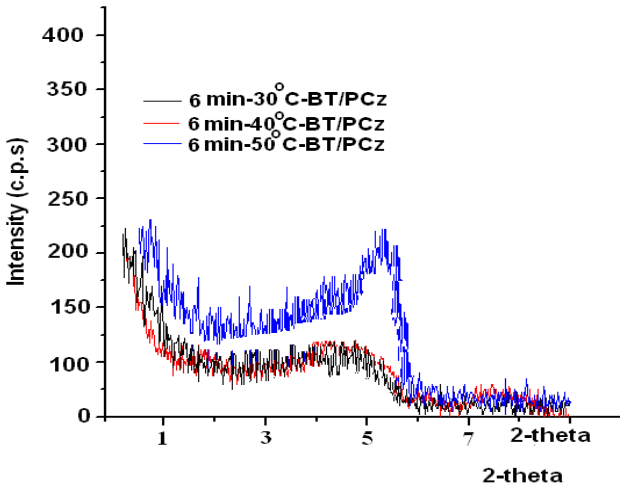

(c)

Fig.2 XRD patterns of (a) 2min-BT/PCz (b) 4min-BT/PCz (c) 6min-BT/PCz

It was observed that as the temperature was increased from 30^0C to 50^0C at 2 min microwave irradiation in the synthesis of the above nanocomposites, the peak intensity decreased from 4305 to 1667 cps, Fig. 2(a). The peak intensity showed the reflections from the planes in question. The increase in the non-uniform strain in the clay lattice with the increase in the temperature of irradiation reduced these reflections. It is noticeable that even 2 min microwave irradiation at 40^0C and 50^0C produces non-uniform strain and stacking disorder in the siloxane layers. The decrease in the reflection intensity of the nanoyhbrids brings forth the effect of longer microwave irradiation on increasing the stacking disorder. For the nanocomposites 6 min-30^0C-BT/PCz, 6 min-40^0C-BT/PCz, and 6 min-50^0C-BT/PCz, the peak intensity was found to be 100, 125, 225 cps., respectively, Fig. 2 (c) . The reflection intensity of these nanocomposites was lower than those prepared at 2 min and 4 min microwave irradiation at these temperatures. This decrease was caused by the increased strain and stacking disorder in the siloxane lattice because of longer microwave irradiation and larger formation of PCz in the clay interlayer space.

The second derivatives of FT-IR spectra of all the nine composites showed peaks of NH vibration in the range of 3000-3500 cm^{-1}. The presence of these peaks confirmed the formation of PCz in the clay galleries. The second derivative of the FT-IR of the nine nanocomposites showed SiO peaks in the range of 950-1200 cm^{-1}. For obtaining the integrated absorption coefficient, the data were replotted in Gaussian fit program in Origin 8.0 software to obtain well formed peaks. The integrated absorption coefficients so calculated are shown in Table 4. We have used them to delineate information about the conformation of PCz chains within the clay galleries.

Table 4 FT-IR spectra of BT/PCz nanocomposites

Nanocomposite	Span of wavelength for peak area calculation	Peak Position (cm^{-1})/ Absorbance	Area cm^{-2} $\int ad\bar{\nu}$
2-min 30^0C- BT/PCz	3800-2900	3417/42.9	517
4-min 30^0C- BT/PCz		3417/30.0	237
6-min 30^0C- BT/PCz		3417/15.1	116
2-min 40^0C- BT/PCz	3800-2900	3417/40.3	353
4-min 40^0C- BT/PCz		3417/27.7	396
6-min 40^0C- BT/PCz		3417/15.1	201
2-min 50^0C- BT/PCz	3800-2900	3417/40.3	312
4-min 50^0C- BT/PCz		3417/27.7	569
6-min 50^0C- BT/PCz		3417/15.1	512

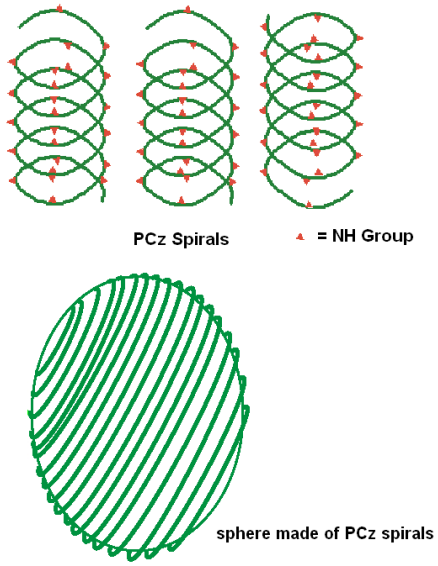

Scheme 1 Formation of PCz Spirals

Table 4 showed that when the microwave irradiation was carried out from 2 min to 6 min at 30^0C the Integrated absorption coefficient, $\int ad\nu$, of NH peak decreased from 517 to 116 cm^{-2}. This decrease was correlated to the shape and orientation of PCz particles in clay galleries. Because of the ease of the turning in of C—C linkage of carbazole monomers, PCz chains can coil around and formed loops which extended into spirals. These spirals reorganized into spheres, when they were taken out of the clay galleries, as was observed under TEM. *Jung et. al.*[29] have found that PCz forms ring shaped macrocycles by the coiling of PCz chains. This has been confirmed by DFT and Force Field Calculations[30]. The hydrophobic interaction between the Cz units of PCz chains impart stability to the spherical structure of PCz.

Different types of distribution of PCz spirals in the clay galleries were inferred from the integrated absorption coefficients of NH vibration peak of these nanocomposites. A number of such spirals oriented vertically back to back, or, away from one another, Scheme 1. In some cases, a large number of PCz spirals were tilted. In some other cases, they formed mixed distribution of vertical and tilted spirals. When all the PCz spirals oriented vertically they pushed up the siloxane layers and gallery height increased noticeably. When PCz spirals stood titled in the galleries, the gallery height increased fairly. A mixed distribution of PCz spirals would bring about increase in the gallery height in between the above two positions. XRD results confirm these observations. If the spirals stood vertically, of the NH groups lying on the loop, some pointed inwardly and some outwardly. Transition dipole moments of the NH group pointing inwardly and opposite to each other would cancel out. Only the transition dipole moments of NH groups pointing outward would add up. As a resul the net transition dipole moment would be low causing extinction coefficient to be low which made the integral adsorption coefficient of vertical orientation of PCz spirals low. Tilted orientation of PCz spirals at different angles caused only partial cancellation of transition dipole moments of the NH groups pointing outward on the loops of the neighbouring spirals. The net transition dipole moment being higher in this case enhanced the extinction coefficient, which consequently led the $\int ad\bar{\nu}$ to be higher in this case. By the same argument, in the mixed distribution of vertical and tilted spirals, $\int ad\nu$ had intermediate values.

The $\int ad\nu$ of the composite 6-min-30^0C-BT/PCz, 116, was comparatively lower than the composite 2-min-30^0C-BT/PCz, 517. The lower value of $\int ad\nu$ in the former case was obtained due to the vertical orientation of PCz spirals.and the higher value of $\int ad\bar{\nu}$ in the latter case resulted from tilted orientation of PCz spirals in this case. Noticeable and small increase in gallery height, respectively, in these nanocomposites was observed from XRD, which confirmed these results. Relatively large integrated absorption coefficient values of 569 and 512 for 4 min-50^0C-BT/PCz and 6min-50^0C-BT/PCz were obtained due to tilted orientations of the PCz spirals. XRD results also showed small increase in gallery height in these cases. For other nanocomposites $\int ad\nu$ values fell between the two extremes indicating that the PCz spirals had mixed orientations. The FT-IR spectral analysis thus yielded information about the coiling of PCz chains and their orientation in the clay galleries.

Molar mass analysis showed that the nanohybrid 2min-30^0C-BT/PCz had the lowest molar mass or the lowest chain size .The number of NH groups per PCz chains would be smaller in this case as compared to the nanohybrids 2min-50^0C-BT/PCz and 4min-50^0C-B/PCz and 6min-50^0C-BT/PCz. But $\int ad\nu$ of the former was larger than the first and comparable with the later two nanohybrids. The number of NH group in PCz molecule/ chain therefore did not influence the $\int ad\nu$ values. The net transition dipole moment obtained after vectorial addition and subtraction of individual transition moments of NH vibration, therefore, govern the $\int ad\nu$ value of these nanocomposites, which showed variation in their values by different orientations of PCz spirals.

The UV-visible spectrum indicated the electronic transition in PCz or BT/PCz nanohybrids synthesized under different conditions of temperature and time, Fig.3. It is interesting that in all the nine composites, the transitions were obtained at 250 nm, 450 nm and 750 nm.

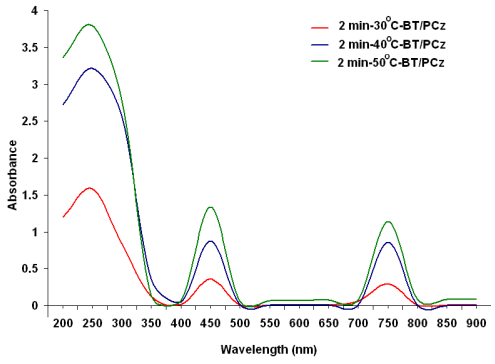

(a)

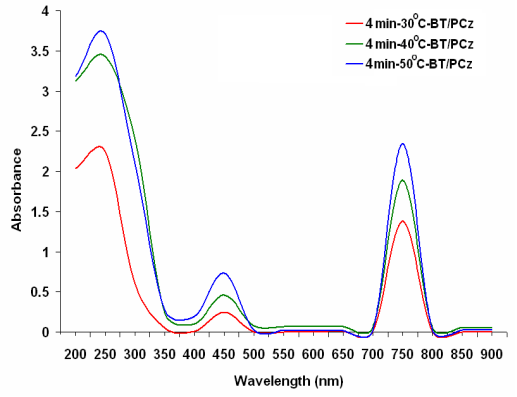

(b)

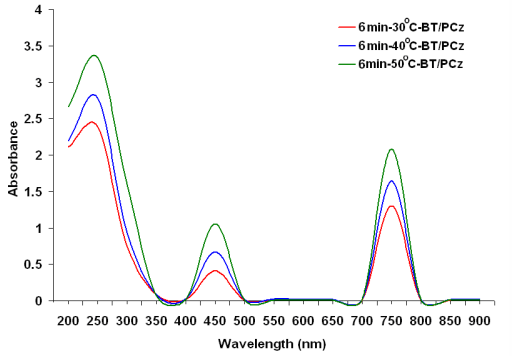

(c)

Fig.3 UV-visible spectra of (a) 2min-BT/PCz, (b) 4min-BT/PCz, (c) 6min-BT/PCz synthesized at different temperatures

The only difference appeared in the different areas under these peaks. The peak at 250 nm arises due to π-π* or inter band transition, the 450 nm peak is attributed to excitonic transition, while the one at 750 nm appears due to polaronic transition; the latter two peaks fall in the inter band region, or, between HOMO and LUMO bands. Several authors have reported that in the undoped state, PCz did not show peaks in the visible region[31-34]. In the undoped state, they appear in the ultraviolet or near ultraviolet region, because of large band gap between HOMO and LUMO[29-32]. Upon doping, PCz shows peaks in the visible region which are attributed to polaron formation. For improving the electronic properties and spectral characteristics of PCz, the latter has been substituted and/or copolymerized using suitable reactants. Films of substituted PCz copolymers poly (2,7-substituted carbazole), synthesized by Leclerc and coworkes and designated as PCDT, PCDTB, PCDTBT [poly(N-9′-heptadecanyl-2,7-carbazole-alt-5,5-(4′,7′-di-2-thienyl-2′,1′,3′-benzothiadiazole)] showed UV-vis absorption peaks at 465 nm; 450 nm; 400 nm and 575 nm[35-36]. Under cyclic voltametry (CV), the same substituted copolymers of PCZ showed peaks respectively at 440 nm and 630 nm; 440 nm and 640 nm; 420 nm, 600 nm, and 790 nm. CV thus introduces polaronic state in substituted PCz through oxidation. These peaks are polaronic and bipolaronic ones lying between HOMO and LUMO band gaps[34]. Interestingly microwave irradiation also produces well formed and suppressed polaronic peaks in the present studies as CV did in the above referred cases. Riaz and Ashraf[26] have earlier reported that PCz synthesis under microwave condition using ferric chloride as an oxidant showed transition peaks at 375 nm, 600 nm, 850 nm and 950 nm. It is therefore a unique property of microwave irradiation to produce polaronic peaks in PCz. The integrated absorption coefficient of the peak of visible transition at 750 nm, in the present case, was used to measure the oscillator strength, which is directly proportional to the $\int ad\bar{\nu}$.

$$f = \int \frac{ad\bar{\nu}}{M}$$

Table 5 Integrated absorption coefficient values of nanohybrids at 750 nm

Nanohybrids	$\int ad\bar{\nu}$ (cm^{-2})	Oscillator strength
2min-30^{0}C- BT/PCz	354	0.0301
2min-40^0- BT/PCz	605	0.0514
2min-50^{0}C- BT/PCz	1214	0.1032
4min-30^{0}C- BT/PCz	1265	0.1075
4min-40^{0}C- BT/PCz	1859	0.1580
4min-50^{0}C- BT/PCz	2213	0.1881
6min-30^{0}C BT/PCz	1207	0.1026
6min-40^{0}C-BT/PCz	1565	0.1330
6min-50^{0}C-BT/PCz	1926	0.1637

Table 5 summarizes the $\int ad\bar{\nu}$ of BT/PCz nanohybrids prepared at different temperatures and microwave irradiation times. The data clearly showed the effect of both the time and temperature of microwave irradiation on the oscillator strength and $\int ad\bar{\nu}$ values of the nanocomposites.

It was observed that for 2 min, 4 min and 6 min microwave irradiation times at each of the temperatures: 30^{0}C, 40^{0}C and 50^{0}C, $\int ad\bar{\nu}$ increases considerably. The increase in $\int ad\bar{\nu}$ with temperature was attributed to the increase in the orbital symmetry of the ground and excited state that also enhances the oscillator strength. This was a significant observation with regard to the effect of temperature on the electronic transition parameter of PCz under microwave irradiation. The $\int ad\bar{\nu}$ value of BT/PCz nanohybrids synthesized at 2 min and 6 min microwave irradiation increased from 354 cm^{-2} to 1207 cm^{-2} at 30^{0}C, from 605 cm^{-2} to 1565 cm^{-2} at 40^{0}C and from 1214 cm^{-2} to 1926 cm^{-2} at 50^{0}C. The increase in the irradiation time thus leads to the enhancement of orbital symmetry of ground and excited states involved in the electronic transition.

Table 5 shows the values of oscillator strength of the nine BT/PCz nanohybrids prepared at 30^{0}C, 40^{0}C and 50^{0}C and exposed to microwave irradiation for 2 min, 4 min and 6 min. The oscillator strength increases as the temperature of synthesis increases from 30^{0}C to 40^{0}C to 50^{0}C whether the BT/PCz nanocomposite was prepared by 2 min, 4 min or 6 min microwave irradiation. It was observed that the increase in oscillator strength from 30^{0}C to 50^{0}C was the highest for 2 min microwave irradiation, 0.0301 to 0.1032, i.e, an increase by 3.4 times. For 4 min microwave irradiation, the oscillator strength increased from 0.1075 to 0.1881, i.e , an increase of 1.7 times as the temperature increased from 30^{0}C to 50^{0}C, and for 6 min time of synthesis, it enhanced from 0.1026 to 0.1637, i.e, an increase by 1.6 times for the same increase of temperature. The increase in

the oscillator strength was found to be the highest, 3.4 times, for 2 min microwave irradiation from 30^0C to 50^0C. The increase in the oscillator strength was slightly low for 6 min synthesis, increasing only 1.6 times. It leads to the conclusion that enhanced orbital symmetry for 2 min microwave irradiation allows highest transition dipole moment that yields highest oscillator strength. The temperature and irradiation time effect on orbital symmetry of the ground and excited states in this case happens to be highest.

Table 5 reveals that when irradiation time is increased from 2 min to 4 min to 6 min at 30^0C, oscillator strength initially increases 3.7 times and then decreases by 3.40 times. At 40^0C, as the time of microwave irradiation was increases from 2 min to 4 min to 6 min, the oscillator strength jumps 3.7 times and then goes down to 2.59 times. The corresponding values at 50^0C were 1.8 and 1.58 times. These results show that increase in the oscillator strength is the highest at 30^0C for 2 min to 4 min microwave irradiation. At 30^0C for 4 min to 6 min microwave irradiation, the increase was 3.4 times which was only slightly lower than the value for 2 min to 4 min microwave irradiation at 30^0C. This reveals that, 30^0C temperature of microwave irradiation leads to the highest increase in oscillator strength. It can therefore be inferred that at any temperature of synthesis, the time of microwave irradiation brings about a larger change in transition dipole moment/orbital symmetry and intensity of polaronic states than the increase in temperature of microwave irradiation does for a particular time.

Interestingly, even the intensity of interband transition at 250 nm changes significantly with increase of temperature and time of microwave irradiation, Table 6. In this case, as the temperature increases from 30^0C to 40^0C to 50^0C for 2 min microwave irradiation, integrated absorption coefficient increases substantially from 24598 cm^{-2} to 56055 cm^{-2} to 64744 cm^{-2}. It reveals that considerable perturbation in HOMO and LUMO orbital occurs which increases the transition probability, enhances transition dipole moment and transition intensity. For 4 min and 6 min microwave irradiation from 30^0C to 50^0C, the corresponding increase in integrated absorption coefficient was comparatively less. It can be inferred that the favorable perturbation in HOMO and LUMO did not occur beyond 2 min microwave irradiation; under the above disposition either small increase in transition dipole moment/ integrated absorption coefficient or a small decrease in these quantities results. These results distinctly show that microwave irradiation brings about perturbation in molecular orbital through temperature and time of irradiation.

Table 6 Integrated absorption coefficient, $\int ad\bar{\nu}$, at 250 nm

Nanocomposites	$\int ad\bar{\nu}$ (cm^{-2})
2min-30^0C-BT/PCz	24,598
2min-40^0C-BT/PCz	56,055
2min-50^0C-BT/PCz	64,744
4min-30^0C- BT/PCz	32,156
4min-40^0C-BT/PCz	58,503
4min-50^0C-BT/PCz	59,451
6min-30^0C- BT/PCz	35,011
6min-40^0C-BT/PCz	39,712
6min-50 ^{0}C-BT/PCz	50,469

Table 7 shows the fluorescence emission intensity of all the nine BT/PCz nanohybrids. The fluorescence intensity increases both with the increase in temperature and time of microwave irradiation. Thus, the synthesis of PCz in the clay galleries at 30^0C, 40^0C, and 50 ^{0}C at 2 min microwave irradiation time enhances the fluorescence intensity of these nannohybrids from 60 to 125 to 185 (a.u.); 4 min irradiation yields fluorescence intensity, respectively, 190, 370, and 460 (a.u.), while for 6 min irradiation the intensity is 270, 500, and 570 (a.u),Fig.4.

Table 7 Emission intensities of nanocomposites

Nanocomposites	Intensity (a.u.)
2min-30^0C-BT/PCz	60
2min-40^0C-BT/PCz	125
2min-50^0C-BT/PCz	185
4min-30^0C- BT/PCz	190
4min-40^0C-BT/PCz	370
4min-50^0C-BT/PCz	460
6min-30^0C- BT/PCz	270
6min-40^0C-BT/PCz	500
6min-50 ^{0}C-BT/PCz	570

It is noticed that the fluorescence emission intensity at any time of microwave irradiation is the highest at 50^0C and lowest at 30^0C ; likewise at any of temperatures 30^0C, 40^0C, and 50^0C, the intensity is lowest for 2 min irradiation and highest for 6 min irradiation. The fluorescence emission intensity depends upon the number of molecules returning to the ground state from the first excited state. The increased orbital symmetry in the ground and excited states in the above cases enhances fluorescence transition dipole moment and fluorescence transition property, which is reflected in higher emission and excitation intensities. The trend of increase in the excitation intensity is the same as in the case of emission intensity, as the temperature and time of microwave irradiation was varied. The fluorescence studies establish that in the synthesis of BT/PCz nanohybrids, molecular orbitals of PCz are favourably perturbed in the ground and excited states. The peak shape for 6 min microwave irradiation at 40^0C and 50^0C is different from those at 2min and 4 min time of irradiation at these temperatures. The peaks appear as sharp half Gaussian curves.

This further indicates that longer time of irradiation perturbs the complexion of the molecular orbitals acutely in the excited state which leads to the abrupt rise to the highest intensity or abrupt decrease to the lowest intensity at the same wavelength.

Since in OLEDs exciton decays by fluorescence and phosphorescence, the increase in fluorescence intensity in PCz, a hole transporting/emitter semiconductor will cause higher radiative decay of excitons and hence will increase the Quantum Efficiency (QE) of the OLED[37]. Exciton decay by phosphorescence through suitable modification in PCz by microwave irradiation is expected to further enhance the QE of OLED. The HOMO level of PCz, calculated after *Kulkarni et al* [38] was found to be 4.6 V. This will further enhance the hole injection and transport in PCz layer which will result in higher QE of OLED. Chemical doping is also found to enhance the QE of organic light emitting diode[39]. But it also reduces the driving voltage of the light emitting device. Chemical doping has a deleterious effect on the hole transport/emitter layer of the OLEDs. As in our case, the polaronic state in PCz is produced by microwave irradiation, it will remain safe from the deleterious effect of a chemical dopant when used as hole transport/emitter layer. Because of these beneficial properties, PCz formed by microwave irradiation needs evaluation for increased quantum efficiency in OLEDs.

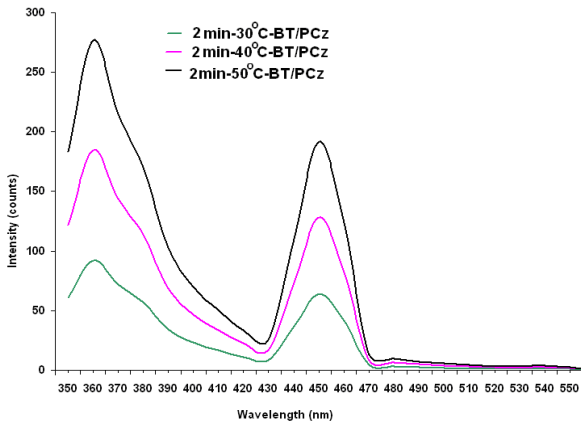

(a)

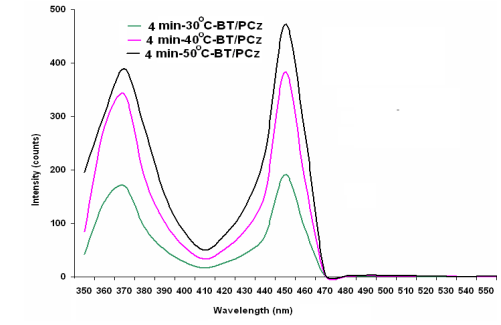

(b)

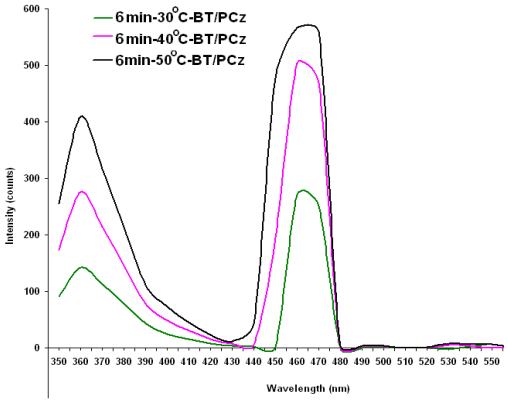

(c)

Fig.4 Fluorescence spectra of (a) 2 min-BT/PCz, (b) 4min-BT/PCz, and (c) 6 min-BT/PCz nanocomposites synthesized at different temperatures

Conclusion

Polymerization of Cz and its in-situ intercalation into bentonite galleries under solid-state conditions by microwave irradiation for 2 min, 4 min, and 6 min at temperatures 30^{0}C, 40^{0}C, and 50^{0}C using ammonium persulphate as initiator led to the attainment of spherical and control sized PCz particles. Integrated absorption coefficient of NH vibrational peaks of the nanocomposites revealed that PCz spirals were formed within the clay galleries with different orientations. Upon extraction from clay galleries , PCz particles of spherical shape of controlled morphology were obtained, the later depending upon the time and temperature of irradiation. Both the time and temperature of irradiation determined the size of the spherical particles; 2 min irradiation at 30^{0}C yielded spherical particles of PCz of the size 50-90 nm and 6 min irradiation at 50^{0}C produced PCz spherical particles of size 300-500 nm. Molar mass of the PCz particles were also governed by the time and temperature of microwave irradiation. Irradiation of 2 min at 30^{0}C yielded molar mass of 3150 Da but irradiation of 6 min at 50^{0}C produced PCz spheres of molar mass of 3888 Da. Microwave irradiation caused time and temperature dependant rapid polymerization of Cz into PCz, i.e., in 2 min at 30^{0}C about 73% conversion of Cz into PCz occured.. UV-visible and fluorescence characteristics of the nanohybrids were strikingly enhanced both by temperature and time of irradiation. By irradiation at 2 min from 30^{0}C to 50^{0}C, the oscillator strength of the peak at 750 nm increased from 0.0301 to 0.1032,equal to 3.43 times and by irradiation at 30^{0}C from 2 min to 6 min the oscillator strength increased from 0.0301 to 0.1026, equal to 3.4 times. In the same manner fluorescence emission intensity was enhanced by increasing the temperature and time of irradiation. By 2 min irradiation from 30^{0}C to 50^{0}C the fluorescence intensity increased from 60 to 185 counts while the irradiation from 2 min to 6 min at 30^{0}C enhanced the fluorescence intensity from 60 to 270 counts, the corresponding increase at 50^{0}C from 2min to 6 min was observed from 185 to 570 counts**.** These parameters can be useful in the designing of LEDs and solar cells based on PCz.

Acknowledgement

The corresponding author Dr.Ufana Riaz also wishes to acknowledge the *Department of Science and technology (DST)-science and engineering research board DST-SERB ,* India vide sanction no SB/S-1/PC-070-2013 for granting major research project". Part of the research work (GPS analysis) was supported by the DST-FIST-2004 Programme of the Department of Chemistry, Jamia Millia Islamia. The corresponding author also wishes to thank the sophisticated analytical instrumentation facility (SAIF) at All India Institute of Medical Sciences (AIIMS) for granting the TEM facility.

References

1. C.O.O.Kappe, Angewandte Chemie Int.Edn., 2004, **43**, 6250.
2. B.A.Roberts, C.R.Strauss, Acc.Chem.Res., 2005, **38**,653.
3. V.Polshettiwar and R.S.Verma, Acc.Chem Res., 200, **841**,629.
4. K.J.Rao, B.Vaidyanathan, M.Ganguli and P.A. Ramakrishnan, Chem.Mater.,1999,**11**, 828.
5. K.Kempe, C.R.Becer and U.Schubert, Macromolecule, 2011, **44**, 5825.
6. A.Sosnik, G.Gotelli, G.A.Abraham,Prog.Polym.Sci., 2011, **36**,1050.
7. C.Sanchez, P.Belleville, M.Popall, and L.Nicole, Chem.Soc.Rev., 2011, **40**,696.
8. D.R.Larson, W.R.Zipfel, R.M.Williams, S.W.Clark, M.P. Bruchez, F.W. Wise, W.W. Webb, Science, 2003, **300**,1434.
9. X.H.Gao, W.C.W.Chan, S.M. Nie,J.Biomed.Opt., 2002,**7**, 532.
10. H.Y.Fan, K.Yang, D.M.Boye, T.Sigmon, K.J.Malloy, H.F.Xu, G.P.Lopez, C.J.Brinker, Science, 2004,**304**, 567.
11. Robert J Cavaa, F.J.DiSalvob, L.E.Brusc, K.R.Dunbard,C.B. Gormane,S.M.Hailef, L.V.Interranteg, J.L. Musfeldth, A. Navrotskyi,R.G.Nuzzoj,W.E.Pickettk,A.P.Wilkinsonl,C.Ahnm , J.WAllenn,P.C.Burnso,G.Cederp,C.E.D.Chidseyq, W.Cleggr, E.Coronados, H.Dait, M.W.Deemu, B.S.Dunnv,G.Galliw, A.J.Jacobsonx, , M.Kanatzidisy,W.Linz, , A.Manthiramaa, M. Mrksichbb, D.Norriscc, A. J.Nozikdd, X.Pengee,C.Rawnff, D. Rolisongg, D.J. Singhhh, , B.H.Tobyii, S.Tolbertjj, U.BWiesnerkk, ,P.M. Woodwardll, P.Yangmm, Prog.Solid State Chem., 2002, **30(1-2)**,1.
12. A.J. Nozik, Physica E, 2002,**14**,115.
13. W.U.Huynh, J.J.Dittmer, W.C.Libby, G.L.Whiting, A.P.Alivisatos, Adv. Funct.Mater., 2003, **13**,73.
14. M-A. De Paoli , W.A.Gazotti, J.Braz.Chem.Soc., 2002, **13(4)**, 410.
15. F.Bergaya, M.Jaber, J.F.Lambert, Environmental Silicate Nano-Biocomposites ,Green Energy and Technology, 2012, 41-75.
16. T.J,Beall, G.W. Pinnvaiva, Polymer-Clay Nanocomposites, Eds.Wiley, West Sussex, England,2000.
17. P.Aranda and E.Ruiz-Hitzky, Chem.Mater.,1992, **4**, 1395.
18. P.Aranda,Y.Mosqueda,E.P.Cappe,E.RuiHitzky, J.Polym.Sci.Part B, Phy., 2003, **41**, 3249.
19. E.Ruiz-Hitzky , P.Aranda , M.Darder and M.Ogawa , Chem.Soc.Rev., 2011, **40**, 801.
20. I.Ahmad, M. Hussain,K-S.Seo, Y-H.Choa, J.Appl.Polym.Sci., 2010, **116(1)**, 314.
21. L.Yang, J-K. Feng, A-M.Ren, J-Z Sun ,Polymer, 2006,**47(4)**,1397.
22. M.Baibarac, M.L.Cantú, J.O.So, I.Baltog, N.C.Pastor, P.G.Romero, Comp.Sci.Technol.,2007, **67(11)**, 2556.
23. M.Łapkowski, P.Data, A.N.Oleksy, J.Sołoducho S.Roszak, ,Mater. Chem.Phy., 2012, **131(3-5),**757.
24. P.Taranekar , T.Fulghum ,A.Baba , D.Patton ,R.Advincula, Langmuir**,** 2007**, 23(2),** 908.
25. J.Li and A.C.Grimsdale, Chem. Soc. Rev.**,** 2010,**39**,2399.
26. U.Riaz and S.M.Ashraf ,J.Phy.Chem.C,2012,**116**,**12366.**
27. J-M Yeh , S-J Liou , C-Y Lai , and P-C Wu, Chem.Mater., 2001, **13(1)**, 1131.
28. D.Lee,K.Char, S.W. Lee and Y.W.Par, J. Mater. Chem., 2003, **13**, 2942–2947
29. S-H Jung, W.Pisula,A.Rouhanipour, H.J-Rader, J. Jacob, K.Mullen, Angew.Chem.Int. Ed., 2006, **45(1)**, 4685.
30. T.Vehoff, J.Kirpatrick, K.Kraemer, and D. Andreiko, Phy.Status.Solidi B, 2008, **245(5)**, 839.
31. S.A. Kumar, A.D.D.Dwivedi, P.Chakrabarti, R.J.Prakash, Appl.Phys. 2009, **105**,114506.
32. S.Grigalevicius, B.Zhang, Z.Xie, M.Forster, U.Scherf, Org.Electron., 2011,**12**, 2253.
33. B.Gupta, R.Prakash, Synth.Met. 2010, **60**,523.
34. G.A.Sotzing, J.L.Reddinger, A.R.Katritzky, J.Soloducho, R.Musgrave, J.R.Reynolds, Chem.Mater., 1997, **9**, 1578.
35. R.B.Aïch, N.Blouin, A.M.Bouchardand, Chem.Mater., 2009, **21**, 751.
36. J-F Morin, N.Drolet, Y.Tao, M.Leclerc, Chem.Mater., 2004, **16**, 4619.
37. B.Geffroy, P.Roy, and C.Prat, Polym Int., 2006, **55**,582.
38. A.P. Kulkarni, C.J. Tonzola, A.Babel, and S.A. Jenekhe, Chem.Mater. , 2004, **16**, 4556.
39. J.Qiu, High Efficiency Organic Light Emitting Diodes with MoO_3 Doped Hole Transport Layer, A thesis submitted to Materials Science & Engineering ,University of Toronto, 2012, 1-60.